

Phosphorus Thermochemistry And MHD Plasma Conductivity

Author(s): J. Wormhoudt, A. Freedman, and C. E. Kolb

Session Name: Plasma Properties and Materials

SEAM: 19 (1981)

SEAM EDX URL: <https://edx.netl.doe.gov/dataset/seam-19>

EDX Paper ID: 904

PHOSPHORUS THERMOCHEMISTRY AND MHD PLASMA CONDUCTIVITY

J. Wormhoudt, A. Freedman, and C.E. Kolb
Aerodyne Research, Inc.
Bedford, MA 01730

Abstract

In response to concern over the negative effect of phosphorus oxide negative ions on coal-fired MHD plasma conductivity, results are presented of predictive modeling of several combustion gas systems in which measurements of potassium and phosphorus species concentrations were measured. Modeling is done with a number of sets of thermodynamic parameters for these species, with the aim of showing that all observations can be simultaneously predicted and are therefore consistent with each other. Those models are then applied to generator performance prediction. Among the conclusions are that phosphorus oxide negative ions may have less effect on MHD plasma conductivity and generator performance than previously predicted, that this is probably due to stable neutral potassium phosphate species, and that the necessary thermochemical parameters for some molecules are still not adequately specified.

1. Introduction

Accurate prediction of the plasma conductivity in open-cycle coal-fired MHD generators has been known for some time to depend on the thermochemical parameters for a number of ash-derived molecular species.¹ The requirement for these thermochemical properties, many of which are quite uncertain, has led to studies which have recently yielded new information on phosphorus species.^{2,3,4} The phosphorus system is of particular interest because its negative ions have been predicted to be the most important in MHD systems, especially at the cool end of the channel.¹

Experimental investigations are continuing, and the state of knowledge for a number of phosphorus species is still not satisfactory. However, thermochemical modeling to assess the implications of existing data and their uncertainties is always useful, if only to show which thermochemical parameters require further study. For this particular system, it is especially interesting to see if all observations made under varying conditions can be modeled with the same set of thermochemical parameters, since initially the observations had been interpreted to yield conflicting values.

To begin, it is appropriate to review the history of phosphorus species modeling in MHD systems. The first observation which was incorporated into modeling of plasma chemistry was that by Miller of the electron affinity of PO_2^- .² The PO_3^- ion was later added to our modeling, with the heat of formation set by the ratio of PO_2^- and PO_3^- concentrations determined by our mass spectrometric observations of combustion gases from a laboratory-scale seeded methane burner, as reported in Reference 4. The predicted effect of both phosphorus oxide ions was to cause substantial reductions in conductivity upon the

addition of phosphorus to an MHD plasma. Recently, Annen and co-workers performed just such phosphorus addition experiments in an ethanol-fueled laboratory scale MHD channel.³ They concluded that phosphorus addition produced a much less severe decrease in conductivity than was predicted by modeling using only oxides as major phosphorus species. They interpreted these observations in terms of lower electron affinities for the phosphorus oxide species, in conflict with the observations of References 2 and 4.

It is a major goal of this paper to show that those observations can also be modeled by retaining large phosphorus oxide electron affinities and including stable potassium phosphate molecules in the species considered. Although it is not surprising that molecules with large electron affinities such as PO_2^- and PO_3^- should form stable alkali compounds, our consideration of such species only began at the suggestion of J.W. Hastie of the National Bureau of Standards (NBS), based on his studies of the lithium and sodium analogs.⁵ Subsequently, Hastie provided us with thermochemical models for both KPO_2 and KPO_3 gas-phase molecules,⁶ with estimated heats of formation based both on an earlier observation in each case,^{7,8} and on analogy to measurements of the sodium species by both the NBS group⁵ and by the authors of References 7 and 8.

Meanwhile, our laboratory burner measurements had been extended to neutral mass spectrometric observations of combustion gases seeded with equal amounts of potassium and phosphorus which showed roughly equal peak heights for KPO_2 , KPO_3 , and KOH under similar conditions to the earlier ion measurements. These observations were reported in Reference 9, along with studies of combustion gases seeded with phosphorus alone. In these latter systems, both References 5 and 9 show PO and HPO_2 as the major species, with Reference 9 also identifying HPO_3 as an important constituent. However, in MHD systems these molecules are of minor importance in comparison to the potassium phosphates, and will not be discussed further here.

We now proceed to assess the adequacy of the present knowledge of PO_2^- , PO_3^- , KPO_2 , and KPO_3 , first by examining the ability of various sets of choices of molecular stabilities to predict all the observations detailed above, and then by calculating theoretical MHD channel performance for several of these sets of assumed thermodynamic parameters. It will be shown that the effect on predicted performance is quite substantial, and that although not all observations can be fit without allowing for fairly large error limits, the present observations set constraints on the thermochemistry of the potassium-phosphorus system. These calculations also establish that previous laboratory studies^{2,3,4} are not in conflict to the extent assumed in previous analyses.³

II. Thermodynamic Data Sets and Observations

We begin by comparing the agreement between the observations of References 2, 3, and 4 and model calculations using the set of heats of formation listed in the first column of Table 1. This data set A is one of a large number of arbitrary sets whose values lie within error bounds of those recommended in either Reference 5 or 8, and which show acceptable agreement with the observations of both Miller² and Annen³ as well as our own.^{4,9} Comparison with data from Miller's flames is given both in Figures 1 and 2 and in Table 2, which also contains comparisons with Annen's and our own mass spectrometric data.

It can be seen that there is a systematic trend in the comparison between model predictions and the data from the four flames. The predicted ratios of negative ion and electron concentrations are much above the observation in the lowest temperature flame, while they are below the observation at the highest temperature. This systematic difference will be encountered by all postulated data sets, so that agreement can only be attained at one point. Although the cause of the trend is not known, it has been suggested that the largest uncertainties arise in the measurement of positive ion concentrations at low temperatures, and that the values obtained using the 2250K flame have been the most reliable, based on agreement of its results with other studies. However, the possibility that a remaining problem in the modeling (such as yet another missing species or a substantially different structure and resulting temperature dependence) is actually indicated cannot be ruled out. In any case, Miller removed the data from the lowest temperature flame from the determination of a PO_2^- heat of formation, and we will also only compare with the other three. It can also be mentioned here that his grounds for disregarding the low temperature data included the upward curvature in the N_-/N_e plot, and that an upward curvature is also seen in the predictions.

With the Set A values, agreement with the Miller data is best at high temperatures, and also clearly quite good with all the Annen observations. (It should be pointed out that the model always predicts no-phosphorus electron concentrations quite well.) PO_3^- to PO_2^- ratios of between 10 and 100 were observed in the work reported in Reference 4, presumably varying with changes in burner stoichiometry. Stoichiometry was at that time not as well known as is desirable. Therefore, the predicted ratio for nominal conditions constitutes quite acceptable agreement. Whether the KOH/KPO_x ratios correspond to the observation of similar mass spectrum peak heights depends on the degree of dissociative ionization which is assumed for each species. KOH has been observed to be relatively stable through mass spectrometric sampling,⁶ and the high degree of cracking observed in molecules like KCl may suggest similar behavior for highly ionic KPO_x species, leaving agreement between prediction and observation at least a possibility.

Heat of formation set B in Table 1 is that suggested by Hastie.⁶ The recommended value for KPO_2 indicates a slightly more stable molecule than did the only direct experiment, the (unspecified) measurement reported in Reference 7.

That for KPO_3 , on the other hand, corresponds to a slightly more stable compound than that implied by the single measurement of Reference 8. The molecular structure for both species was also estimated by Hastie, based on spectroscopic studies by I. Beattie, and the resulting entropies and heat capacities are used in all modeling reported here. (A good discussion of the knowledge of the structure of PO_2^- is contained in Reference 10, and this information is incorporated into the present modeling.) The same comparisons with observation, in Table 3, now show that the KPO_3 model is so stable that very little effect would have been seen by Annen upon addition of even large amounts of phosphorus, while the KPO_x models still allow too many negative ions under Miller's conditions. The large ratio of KPO_3 to KPO_2 is not necessarily in conflict with our observation of similar mass spectrum peak heights, since KPO_2 could result simply from cracking of KPO_3 in the electron impact ionizer.

Hastie assigns uncertainties of ± 10 kcal/mole to both the KPO_2 and KPO_3 heats of formation, while Miller quoted ± 0.3 eV (± 6 kcal/mole) limits for PO_2^- , and error limits for PO_3^- are larger still. As will become clear as more cases are considered, there are two ways to improve agreement with Annen's data - in this case either lowering the neutral stabilities or raising those of the ions. Modified parameter sets C and D in Table 1 give examples of each option, with Set C decreasing the stability of KPO_3 by slightly more than the estimated error bounds, and Set D increasing the PO_2^- stability by the 6 kcal/mole error limit (as will be explained below, this does not, however, necessarily bring PO_2^- to its limiting stability.)

The results of model predictions using these two sets of values are given in Tables 4 and 5. It can be seen that Set C still shows too little effect upon phosphorus addition with respect to both Annen and high temperature Miller data. Although only a slight further reduction in KPO_3 stability would result in good agreement with Annen, only a stronger PO_2^- would improve agreement with Miller. On the other hand, Set D shows slightly too many predicted negative ions in comparison to the Miller 2250K flame data, while still not showing enough in the Annen systems. At this point it must be mentioned that one reanalysis of Miller's experiments using the final value of the HPO_2 heat of formation chosen by Hastie⁴ would result in a PO_2^- heat of formation which is more stable by 8 kcal/mole. Therefore, even the -152 kcal/mole value (4 eV electron affinity) is not necessarily too high. It also should be pointed out here that the much higher equivalence ratios (1.7 to 2.0) used by Miller (versus 0.9 used by Annen) favor PO_2^- and KPO_2 over PO_3^- and KPO_3 . Thus one way to obtain better agreement is seen to be an increase in KPO_2 stability (temporarily lowering the negative ions predicted in Miller's systems) coupled with either a further increase in PO_2^- stability or a further decrease in KPO_3 stability (thereby raising all predicted negative ion levels).

One set of heats of formation which does move in this direction is that denoted by Set E in Table 1, which is that suggested in Reference 9. As detailed there, the KPO_2 and KPO_3

values are chosen entirely by analogy to other compounds. The comparisons in Table 6 show that this set results in the prediction of too many negative ions under Annen's conditions, too few in Miller's high temperature flames, and too many at low temperatures. It turns out that one way to improve agreement with both Annen and the Miller high temperature data is to increase the stability of all four species, but to make larger increases in the stability of the neutral species. Changes in this direction resulted in the otherwise arbitrary values of Set A, whose good agreement with both sets of data has already been demonstrated.

A final point to be investigated is raised by the observation that Annen's experiment did not provide direct information about phosphorus negative ion stabilities, but only on the relative stabilities of the ions and the potassium phosphate neutrals. It is of interest to lower all stabilities by an equal amount, and see if the result of the competition is the same. Therefore, in Set F of Table 1, all the Set A heats of formation have been reduced by 15 kcal/mole. The comparisons in Table 7 show that agreement with Annen's observations remains quite satisfactory. However, comparison to Miller's observations shows the PO_2^- stability to be much too low. Considering that it was designed to produce data on the PO_2^- ion, it is not surprising that Miller's experiment should be quite sensitive to its heat of formation. What is worthy of note is that Annen's experimental conditions are such that his measurements were not sensitive to negative ion heats of formation, but only to the relative stabilities of PO_x^- and KPO_x species.

III. Predictions of Theoretical MHD Channel Performance

Annen's experimental conditions have the virtue that they are closer (especially in terms of stoichiometry and seed loading) to conditions in an MHD channel than were Miller's. However, there remains a gap to be bridged using predictive modeling, since, for instance, even higher temperatures than those investigated by Annen are encountered in a real channel. As another consideration, MHD combustors are typically operated slightly fuel rich (to minimize NO concentrations), while Annen ran under slightly lean conditions, intending to promote PO_x^- formation. Therefore, in this section we present results of MHD channel performance calculations for parameter sets A, C, and E, as well as for set E with KPO_2 and KPO_3 omitted from consideration, which corresponds to the system used in our more recent previous modeling studies.¹ The inputs to the generator model are those for the 20% oxygen enriched case used in those earlier studies,^{1,11} which is similar to the ETF design in many respects, but contains some features leading to shorter channels (and shorter computation times) for a desired fractional enthalpy extraction. These inputs are displayed in Table 8, and more discussion can be found in References 1 and 11.

To give an idea of the temperature range involved, Figure 3 shows the temperature history for the nominal generator and the phosphorus thermodynamic input data set A in Table 1. As will be seen, this set gives the highest plasma

conductivity and largest enthalpy extraction of the parametric cases considered here, and therefore the other temperature drops in the same channel length are smaller.

The fact that more efficient (due to higher conductivity, for example) generators extract energy in shorter channel lengths, leading to lower downstream temperatures (and eventually lower conductivity), must be kept in mind in considering Figure 4, which presents conductivity histories for all four parametric calculations. As mentioned before, Set A with very stable values for both KPO_2 and KPO_3 has the highest initial conductivity, but by the above comment the conductivity curve eventually drops below the others due to the larger temperature drop. Set E, with less stable KPO_x species, results in a lower conductivity except at the low temperature end. Set C, which also agrees well with Annen's observations in the 2200 - 2400K range, is seen to have a yet lower initial conductivity. This is because Set C depends on a very stable KPO_3 alone to reduce the phosphorus negative ion concentrations, and KPO_3 is less stable at higher temperatures than the KPO_2 which contributes to the chemistry in the other two sets. Finally, by far the lowest conductivity is predicted by using Set E but omitting KPO_2 and KPO_3 from consideration. This corresponds to the thermodynamic set used in earlier parametric studies.^{1,11}

Finally, Figure 5 shows how these differences in conductivity are translated into fractional enthalpy extraction predictions. As expected, that based on Set A is the most efficient generator. However, by the downstream end of the channel Set C is doing a bit better than Set E, because at lower temperatures the benefits of increased KPO_3 in Set C more than offset those of increased KPO_2 at the high temperature end for Set E. Ignoring the existence of KPO_x molecules while retaining PO_x^- ions is seen to give very significantly lower performance.

Figures 6 through 9 show, for each case, the concentrations of the various species which contribute to the conductivity prediction. As yet a further speculation, a stable $KFeO_2$ gas phase molecule was included, but it turns out that it has little effect on the FeO_2^- concentration, as the major iron species are quite stable liquid phases.

IV. Conclusions

The lessons of this study are threefold. First, the observations by Annen of small effects of added phosphorus in heavily potassium-seeded plasmas are by no means inconsistent with even a higher electron affinity for PO_2 than that determined by Miller under low potassium, fuel-rich conditions. On the contrary, there is a body of evidence for the existence of stable potassium phosphate species which allow both observations to co-exist. Second, the existence of these potassium phosphate species means that predicted plasma conductivities and efficiencies for coal-fired open-cycle MHD generators should be substantially larger than would have been obtained with the thermodynamic inputs used to date. Finally, it was seen that the observations discussed here do not unambiguously define all of the key molecular properties, although they do provide constraints. Therefore, significantly

different performances may be predicted using equally justifiable sets of parameters, and more experimental work is indicated to better define the properties of both the ions and neutrals.

Finally, uncertainties in negative ion formation effects on coal combustion plasma conductivity is not limited to phosphorus. Serious gaps in our knowledge of thermochemical parameters for iron and aluminum oxide species also limit our current predictive capability.¹

Acknowledgments

This work was supported by the Office of Magnetohydrodynamics of the U.S. Department of Energy under Contract No. EX-76-C-01-2478. The authors would like to thank Drs. J.W. Hastie, W.J. Miller, and K.D. Annen for their helpful discussions.

References

1. Wormhoudt, J., Yousefian, V., Weinberg, M., Kolb, C.E., Sluyter, M.M., "A Review of Plasma Chemical Considerations in MHD Generator Design," at the 7th International Conference on MHD Electrical Power Generation, M.I.T., Cambridge, MA, June 1980.
2. Miller, W., J. Chem. Phys. 1978, p. 3709,69.
3. Annen, K.D., Kuzmenko, P.J., Keating, R., Self, S.A., "Comparative Measurements of Electron and Positive Ion Concentrations in Combustion Plasmas With Application to the Effect of Phosphorus Negative Ions and Plasma Conductivity," at the 7th International Conference on MHD Electrical Power Generation, M.I.T., Cambridge, MA, June 1980.
4. Wormhoudt, J., Kolb, C.E., "Mass Spectrometric Determination of Negative and Positive Ion Concentrations in Coal-Fired MHD Plasma," in Proceedings of the 10th Materials Research Symposiums on Characterization of High Temperature Vapors and Gases, NBS Special Publication 561, October 1979, National Bureau of Standards, p. 57.
5. Hastie, J.W., Bonnell, D.W., "Molecular Chemistry of Inhibited Combustion Systems," National Bureau of Standards 1980, NBSIR 80-2169.
6. Hastie, J.W., private communication, September 1980.
7. Smoes, S., and Drowart, J., Faraday Symposium No. 8, 1973, p. 139.
8. Steblevskii, A.V., Alikhanyan, A.S., Sokolova, I.D., and Gorgoraki, V.I., Russian Journal of Inorganic Chemistry 22, 11, 1977.
9. Freedman, A., Wormhoudt, J.C. and Kolb, C.E., "Studies of Phosphorus Chemistry Important to MHD Combustion," presented at ACS High Temperature Symposium, Atlanta GA, April 1981.
10. Hunter, S.J., Hipps, K.W., and Francis, A.H., Chemical Physics 39 209, 1979.
11. Wormhoudt, J.C., Kolb, C.E., Yousefian, V., and Martinez-Sanchez, M., "Studies of MHD Generator Performance with Oxygen Enriched Coal Combustion," Paper 80-1343, AIAA 13th Fluid and Plasma Dynamics Conference, Snowmass, CO, July 1980.

TABLE 1 - HEAT OF FORMATION DATA SETS FOR KEY PHOSPHORUS SPECIES (KCAL/MOLE)

	A	B	C	D	E	F
KPO ₂	-150	-113	-113	-113	-135	-135
KPO ₃	-200	-217.5	-205	-215	-195	-185
PO ₂ ⁻	-150	-146	-146	-152	-146	-135
PO ₃ ⁻	-215	-211	-211	-211	-211	-200

TABLE 2. COMPARISONS BETWEEN PHOSPHORUS ION OBSERVATIONS AND PREDICTIONS USING HEAT OF FORMATION SET A

ANNEN ³		MILLER ¹	
$N_2/O_2 = 1.4, 2274^\circ K$		$H_2/N_2/O_2 = 4/4/1, 2020^\circ K$	
MOLE FRACTION P(10 ⁻⁵)	3.2	31	MOLE FRACTION P(10 ⁻⁶) 2.0 8.0
OBSERVED $N_E(10^{19}M^{-3})$	1.46	0.82	OBSERVED N_-/N_E 0.5 2.0
PREDICTED $N_E(10^{19}M^{-3})$	1.35	0.81	PREDICTED N_-/N_E 1.07 5.4
$N_2/O_2 = 1.0, 2388^\circ K$		$H_2/N_2/O_2 = 3.5/3/1, 2250^\circ K$	
MOLE FRACTION P(10 ⁻⁵)	3.8	30	MOLE FRACTION P(10 ⁻⁶) 2.0 8.0
OBSERVED $N_E(10^{19}M^{-3})$	3.2	2.19	OBSERVED N_-/N_E 0.3 1.25
PREDICTED $N_E(10^{19}M^{-3})$	3.1	2.02	PREDICTED N_-/N_E 0.4 1.6
$1800^\circ K, \phi=1.0$ BURNER MODELING ^{2,8}		$H_2/N_2/O_2 = 3.4/2/1, 2475^\circ K$	
PO ₃ /PO ₂ = 18/1			MOLE FRACTION P(10 ⁻⁶) 2.0 8.0
KPO ₂ /KPO ₃ /KOH = 1/1/0.015			OBSERVED N_-/N_E 0.15 0.55
			PREDICTED N_-/N_E 0.09 0.30

TABLE 3. COMPARISONS BETWEEN PHOSPHORUS ION OBSERVATIONS AND PREDICTIONS USING HEAT OF FORMATION SET B

ANNEN ³		MILLER ¹	
$N_2/O_2 = 1.4, 2274^\circ K$		$H_2/N_2/O_2 = 4/4/1, 2020^\circ K$	
MOLE FRACTION P(10 ⁻⁵)	3.2	31	MOLE FRACTION P(10 ⁻⁶) 2.0 8.0
OBSERVED $N_E(10^{19}M^{-3})$	1.46	0.82	OBSERVED N_-/N_E 0.5 2.0
PREDICTED $N_E(10^{19}M^{-3})$	1.52	1.48	PREDICTED N_-/N_E 2.1 31
$N_2/O_2 = 1.0, 2388^\circ K$		$H_2/N_2/O_2 = 3.5/3/1, 2250^\circ K$	
MOLE FRACTION P(10 ⁻⁵)	3.8	30	MOLE FRACTION P(10 ⁻⁶) 2.0 8.0
OBSERVED $N_E(10^{19}M^{-3})$	3.2	2.19	OBSERVED N_-/N_E 0.3 1.25
PREDICTED $N_E(10^{19}M^{-3})$	3.33	3.15	PREDICTED N_-/N_E 0.66 2.7
$1800^\circ K, \phi=1.0$ BURNER MODELING ^{2,8}		$H_2/N_2/O_2 = 3.4/2/1, 2475^\circ K$	
PO ₃ /PO ₂ = 14/1			MOLE FRACTION P(10 ⁻⁶) 2.0 8.0
KPO ₂ /KPO ₃ /KOH = $3 \times 10^{-7}/1/1.0 \times 10^{-3}$			OBSERVED N_-/N_E 0.15 0.55
			PREDICTED N_-/N_E 0.20 0.76

TABLE 4. COMPARISONS BETWEEN PHOSPHORUS ION OBSERVATIONS AND PREDICTIONS USING HEAT OF FORMATION SET C

ANNEN ³		MILLER ¹	
$N_2/O_2 = 1.4, 2274^\circ K$		$H_2/N_2/O_2 = 4/4/1, 2020^\circ K$	
MOLE FRACTION $P(10^{-5})$	3.2 31	MOLE FRACTION $P(10^{-6})$	2.0 8.0
OBSERVED $N_E(10^{19}M^{-3})$	1.46 0.82	OBSERVED N_-/N_E	0.5 2.0
PREDICTED $N_E(10^{19}M^{-3})$	1.33 1.03	PREDICTED N_-/N_E	0.81 3.2
$N_2/O_2 = 1.0, 2388^\circ K$		$H_2/N_2/O_2 = 3.5/3/1, 2250^\circ K$	
MOLE FRACTION $P(10^{-5})$	3.8 30	MOLE FRACTION $P(10^{-6})$	2.0 8.0
OBSERVED $N_E(10^{19}M^{-3})$	3.2 2.19	OBSERVED N_-/N_E	0.3 1.25
PREDICTED $N_E(10^{19}M^{-3})$	3.17 2.24	PREDICTED N_-/N_E	0.21 0.80
1800°K, $\phi=1.0$ BURNER MODELING ^{2,8}		$H_2/N_2/O_2 = 3.4/2/1, 2475^\circ K$	
$PO_3/PO_2 = 14/1$		MOLE FRACTION $P(10^{-6})$	2.0 8.0
$KPO_2/KPO_3/KOH = 1 \times 10^{-5}/1/6 \times 10^{-3}$		OBSERVED N_-/N_E	0.15 0.55
		PREDICTED N_-/N_E	0.06 0.15

TABLE 5. COMPARISONS BETWEEN PHOSPHORUS ION OBSERVATIONS AND PREDICTIONS USING HEAT OF FORMATION SET D

ANNEN ³		MILLER ¹	
$N_2/O_2 = 1.4, 2274^\circ K$		$H_2/N_2/O_2 = 4/4/1, 2020^\circ K$	
MOLE FRACTION $P(10^{-5})$	3.2 31	MOLE FRACTION $P(10^{-6})$	2.0 8.0
OBSERVED $N_E(10^{19}M^{-3})$	1.46 0.82	OBSERVED N_-/N_E	0.5 2.0
PREDICTED $N_E(10^{19}M^{-3})$	1.50 1.16	PREDICTED N_-/N_E	7.35 12.6
$N_2/O_2 = 1.0, 2388^\circ K$		$H_2/N_2/O_2 = 3.5/3/1, 2250^\circ K$	
MOLE FRACTION $P(10^{-5})$	3.8 30	MOLE FRACTION $P(10^{-6})$	2.0 8.0
OBSERVED $N_E(10^{19}M^{-3})$	3.2 2.19	OBSERVED N_-/N_E	0.3 1.25
PREDICTED $N_E(10^{19}M^{-3})$	3.30 2.90	PREDICTED N_-/N_E	0.69 2.80
1800°K, $\phi=1.0$ BURNER MODELING ^{2,8}		$H_2/N_2/O_2 = 3.4/2/1, 2475^\circ K$	
$PO_3/PO_2 = 14/1$		MOLE FRACTION $P(10^{-6})$	2.0 8.0
$KPO_2/KPO_3/KOH = 2 \times 10^{-5}/1/4 \times 10^{-3}$		OBSERVED N_-/N_E	0.15 0.55
		PREDICTED N_-/N_E	0.13 0.44

TABLE 6. COMPARISONS BETWEEN PHOSPHORUS ION OBSERVATIONS AND PREDICTIONS USING HEAT OF FORMATION SET E

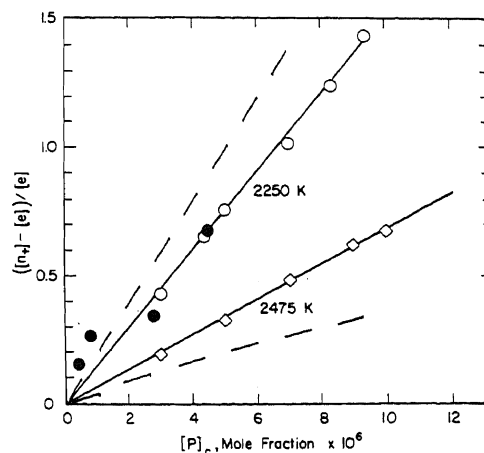
ANNEN ³		MILLER ¹	
$N_2/O_2 = 1.4, 2274^\circ K$		$H_2/N_2/O_2 = 4/4/1, 2020^\circ K$	
MOLE FRACTION $P(10^{-5})$	3.2 31	MOLE FRACTION $P(10^{-6})$	2.0 8.0
OBSERVED $N_E(10^{19}M^{-3})$	1.46 0.82	OBSERVED N_-/N_E	0.5 2.0
PREDICTED $N_E(10^{19}M^{-3})$	1.14 0.50	PREDICTED N_-/N_E	0.78 3.2
$N_2/O_2 = 1.0, 2388^\circ K$		$H_2/N_2/O_2 = 3.5/3/1, 2250^\circ K$	
MOLE FRACTION $P(10^{-5})$	3.8 30	MOLE FRACTION $P(10^{-6})$	2.0 8.0
OBSERVED $N_E(10^{19}M^{-3})$	3.2 2.19	OBSERVED N_-/N_E	0.3 1.25
PREDICTED $N_E(10^{19}M^{-3})$	2.7 1.26	PREDICTED N_-/N_E	0.19 0.74
1800°K, $\phi=1.0$ BURNER MODELING ^{2,8}		$H_2/N_2/O_2 = 3.4/2/1, 2475^\circ K$	
$PO_3/PO_2 = 14/1$		MOLE FRACTION $P(10^{-6})$	2.0 8.0
$KPO_2/KPO_3/KOH = 1/0.4/0.05$		OBSERVED N_-/N_E	0.15 0.55
		PREDICTED N_-/N_E	0.04 0.13

TABLE 7. COMPARISONS BETWEEN PHOSPHORUS ION OBSERVATIONS AND PREDICTIONS USING HEAT OF FORMATION SET F

ANNEN ³		MILLER ¹	
$N_2/O_2 = 1.4, 2274^\circ K$		$H_2/N_2/O_2 = 4/4/1, 2020^\circ K$	
MOLE FRACTION $P(10^{-5})$	3.2 31	MOLE FRACTION $P(10^{-6})$	2.0 8.0
OBSERVED $N_E(10^{19}M^{-3})$	1.46 0.82	OBSERVED N_-/N_E	0.5 2.0
PREDICTED $N_E(10^{19}M^{-3})$	1.36 0.83	PREDICTED N_-/N_E	0.06 0.21
$N_2/O_2 = 1.0, 2388^\circ K$		$H_2/N_2/O_2 = 3.5/3/1, 2250^\circ K$	
MOLE FRACTION $P(10^{-5})$	3.8 30	MOLE FRACTION $P(10^{-6})$	2.0 8.0
OBSERVED $N_E(10^{19}M^{-3})$	3.2 2.19	OBSERVED N_-/N_E	0.3 1.25
PREDICTED $N_E(10^{19}M^{-3})$	3.14 2.12	PREDICTED N_-/N_E	0.03 0.08
1800°K, $\phi=1.0$ BURNER MODELING ^{2,8}		$H_2/N_2/O_2 = 3.4/2/1, 2475^\circ K$	
$PO_3/PO_2 = 18$		MOLE FRACTION $P(10^{-6})$	2.0 8.0
$KPO_2/KPO_3/KOH = 1/1/0.13$		OBSERVED N_-/N_E	0.15 0.55
		PREDICTED N_-/N_E	0.03 0.04

TABLE 8. BASELINE COMBUSTOR/GENERATOR PROPERTIES

COAL:	MONTANA ROSEBUD SUBBITUMINOUS
OXIDIZER:	AIR WITH 20% BY VOLUME O_2 ENRICHMENT (N_2 0.618 MASS FRACTION, O_2 0.371 MASS FRACTION), PREHEATED TO 866°K
SEED:	DRY K_2CO_3 , 1% BY WEIGHT OF TOTAL FLOW
COMBUSTOR STOICHIOMETRIC RATIO (O/F)	0.92
COMBUSTOR PRESSURE:	4.5 ATM.
FIRST STAGE COMBUSTOR TEMPERATURE:	2838°K
SLAG REJECTION FRACTION - (AT FIRST STAGE)	0.85
SECOND STAGE COMBUSTOR TEMPERATURE (AFTER SEED ADDITION)	2807°K
CHANNEL INLET PRESSURE	3.15 ATM.
CHANNEL INLET TEMPERATURE	2715°K
CHANNEL INLET MACH NUMBER	0.80
MAGNETIC FIELD STRENGTH	6 TESLA INITIALLY, LIMITED BY 2100 V/M AXIAL FIELD
LOAD FACTOR	0.80
CHANNEL LENGTH	10M

Figure 1. Comparison of observed (solid lines) ² and predicted (dashed lines) ratios of negative ions to electrons in $H_2/O_2/N_2$ flames at 2250 and 2475 K.

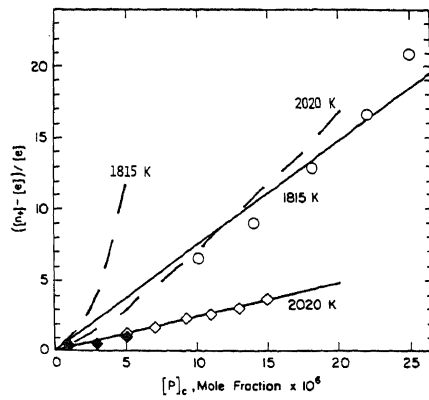


Figure 2. Comparison of Observed (solid lines) and Predicted (dashed lines) Ratios of Negative Ions to Electrons in $\text{H}_2/\text{O}_2/\text{N}_2$ Flames at 1815 and 2020 K.

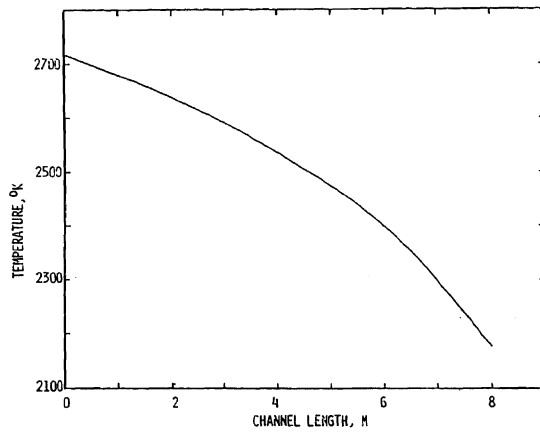


Figure 3. Temperature History Down Channel of Nominal MHD Generator Using Phosphorus Thermodynamic Parameter Set A.

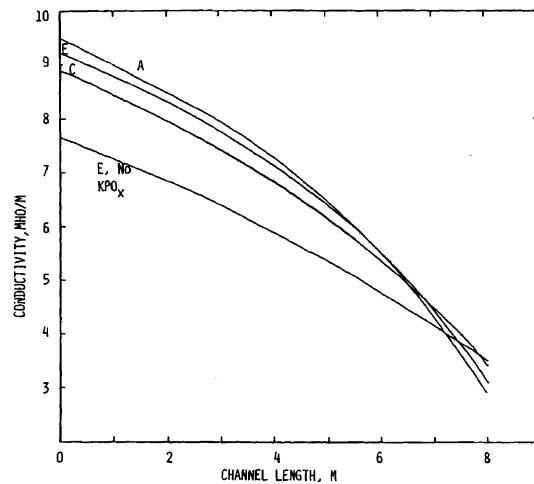


Figure 4. Conductivity Down Channel for Four Different Phosphorus Thermodynamic Parameter Sets.

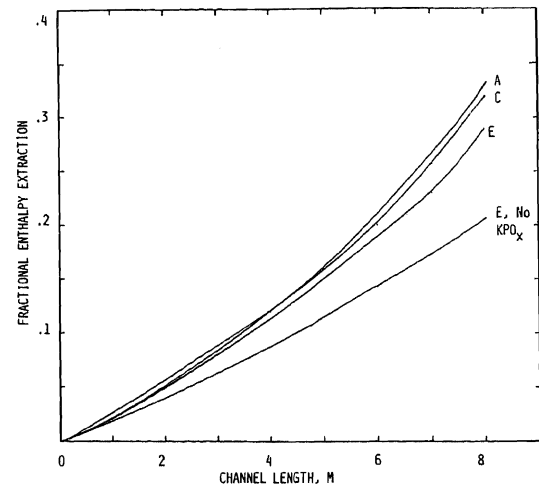


Figure 5. Enthalpy Extraction Down Channel for Four Different Phosphorus Thermodynamic Parameter Sets.

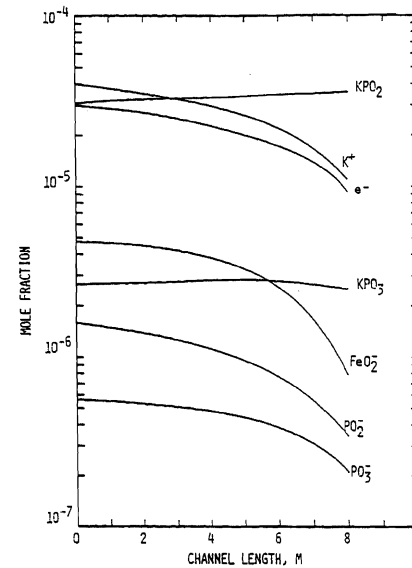


Figure 6. Species Mole Fractions Down Channel for Nominal Generator Using Phosphorus Thermodynamic Parameter Set A.

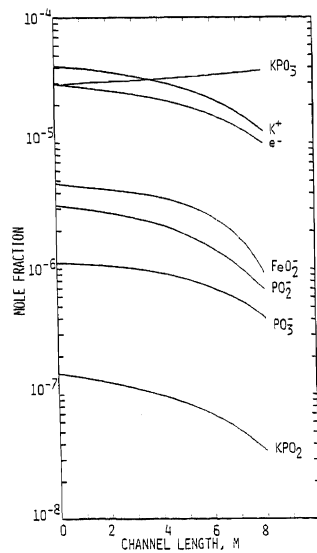


Figure 7. Species Mole Fractions Down Channel for Nominal Generator Using Phosphorus Thermodynamic Parameter Set C.

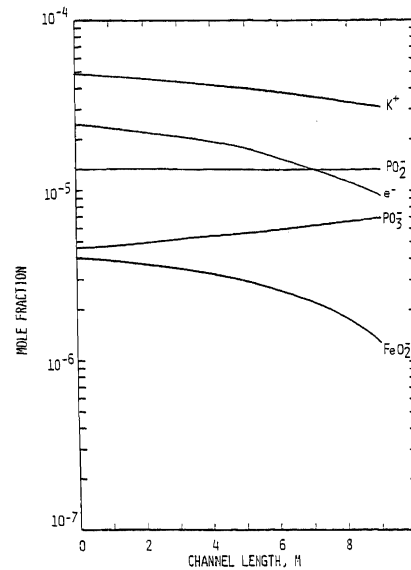


Figure 9. Species Mole Fraction Down Channel for Nominal Generator Using Phosphorus Thermodynamic Parameter E but omitting KPO_2 and KPO_3 .

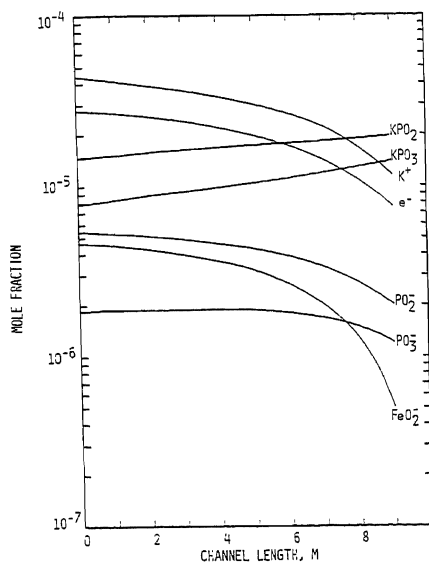


Figure 8. Species Mole Fractions Down Channel for Nominal Generator Using Phosphorus Thermodynamic Parameter Set E.